



Density limits in helium plasmas at JET

J. Rapp^{a,*}, A. Huber^a, L.C. Ingesson^b, S. Jachmich^c, G.F. Matthews^d,
V. Philipps^a, R. Pitts^e, Contributors to the EFDA-JET work programme¹

^a Institut für Plasmaphysik, Forschungszentrum Jülich GmbH, EURATOM Association, TEC, Jülich 52425, Germany

^b FOM Instituut voor Plasmafysica Rijnhuizen, EURATOM Association, TEC, 3430 BE Nieuwegein, The Netherlands

^c ERM/KMS, EURATOM Association, TEC, B – 1000 Brussels, Belgium

^d UKAEA/Fusion Association, Culham Science Centre, Abingdon, OXON, OX14 3EA, UK

^e CRPP Lausanne Centre de Recherches en Physique des Plasmas, Association EURATOM-Switzerland, EPFL, CH – 1015 Lausanne, Switzerland

Abstract

Recently at JET a pure helium campaign has been performed. The exploration of the density limit in L-mode limiter as well as L-mode and H-mode diverted plasmas was one of the main objectives. In L-mode plasmas the density can be increased until the total radiated power equals the heating power, hence the density limit is determined by a radiative collapse. When compared to deuterium plasmas the L-mode density limit in helium is twice as high. In H-mode no significant difference in the density limit process has been observed. The pedestal density just before the H to L-mode back transition is the same in deuterium and helium plasmas. The H to L-mode back transition is followed by a development of a MARFE [J. Nucl. Mater. 145–147 (1987) 15] which eventually leads to a density limit disruption.

© 2003 Elsevier Science B.V. All rights reserved.

Keywords: Operational limits; Divertor; Boundary plasmas; Helium

1. L-mode density limit

For the characterisation of the L-mode density limit, ohmic limiter plasmas, diverted auxiliary heated plasmas with a high and low clearance to the main chamber wall were investigated.

The ohmic limiter plasma leads as in the deuterium case to a poloidally symmetric radiative collapse, meaning the radiated power equals the heating power. But the density limit is more than twice as high than in the deuterium reference case, which is not explained by a different impurity behaviour. The impurity content is even slightly higher in helium pulses, when compared to deuterium for the same density. This is due to stronger physical sputtering of carbon at the limiters. The main

difference of helium from deuterium is the change in the resistivity η_{\parallel} when the density limit is approached. This results in an improved ohmic heating, which allows to increase the density further until the radiation power ($P_{\text{rad}} = C_I n_b^2 (Z_{\text{eff}} - Z_M) + C_M n_b^2$) equals the heating power ($P_{\text{heat}} \propto I_p^2 \eta_{\parallel}$). Here, Z_M is the charge of the main ions, C_I is a constant representing the radiation function of the impurity (in our case: carbon) and C_M is a constant representing the radiation function of the main ions and n_b is the electron density in the plasma boundary. For the resistivity we assume that $T_e \propto P_{\text{heat}} \times \tau_e / n_e$ with $\tau_e \propto I_p^{0.96} \times P_{\text{heat}}^{-0.73} \times M^{0.2}$ taken from the ITER power law regression fit [2]. After some algebra this leads to an expression of the density for the radiative collapse:

$$n_b = A \frac{I_p^{1.08}}{M^{0.6}} \left(\frac{N(Z_{\text{eff}}) Z_{\text{eff}} \ln A}{C_I (Z_{\text{eff}} - Z_M) + C_M} \right)^2 \quad (1)$$

with the resistivity factor $N(Z_{\text{eff}})$ [3]. The term C_M is much smaller than C_I and can be neglected for the

* Corresponding author. Fax: +44-1235 464415.

E-mail address: jurgen.rapp@jet.efda.org (J. Rapp).

¹ See Appendix of J. Pamela et al., in Proceedings of 18th IAEA Fusion Energy Conference, Sorrento, 2000.

following considerations. Changing the main gas from deuterium to helium increases the Z_{eff} from 1.6 to 2.6, which leads to an increase of n_b by a factor of 1.5. This is in relative good agreement with the experiment, which showed an increase of the density in the plasma boundary at the density limit by factor 1.7. The line-averaged density increases by a factor of 2.4 due to a peaked density profile in the helium discharge.

For the L-mode diverted density discharges a comparison for high clearance configurations is shown in Fig. 1(b) (fuelling from inner divertor). In deuterium at 70–80% radiative power fraction the X-point MARFE forms. For He density limit discharges a clear onset of an X-point MARFE is not always detectable (for low heating powers less than for high heating powers). The radiation front moves from the divertor region inside the last closed flux surface (LCFS), which determines the onset of X-point MARFE, at a radiative power fraction of $\approx 80\%$. This happens at a density $\bar{n}_e^{\text{XPM}} = 5.1 \times 10^{19} \text{ m}^{-3}$, which is approximately 40% higher than that in deuterium. At this time the outer divertor is still at-

tached. However, since helium is a strongly recycling element, the fuelling rates, when fuelled from the divertor are not comparable. It is more appropriate to compare the helium density limit discharge, in which the fuelling from the inner divertor is negligible, to a deuterium density limit discharge (#53086), which was fuelled from the main chamber. For those two cases the X-point MARFE forms at similar $q_{\perp} \approx 0.005 \text{ MW/m}^2$. Puffing from the main chamber does allow higher densities before the X-point MARFE develops [4], which means that \bar{n}_e^{XPM} in the deuterium discharge is only 15% below \bar{n}_e^{XPM} in helium.

In deuterium the density can be further increased up to the onset of the inner wall MARFE. For helium the behaviour is totally different. The density can be increased up to 100% radiative power fraction, which happens to be at a 70% higher density ($8.6 \times 10^{19} \text{ m}^{-3}$). No inner wall MARFE forms, the radiation pattern is poloidally symmetric until the radiative collapse. Similar to the limiter density limit discharge in the diverted density limit discharge the ohmic power also increases

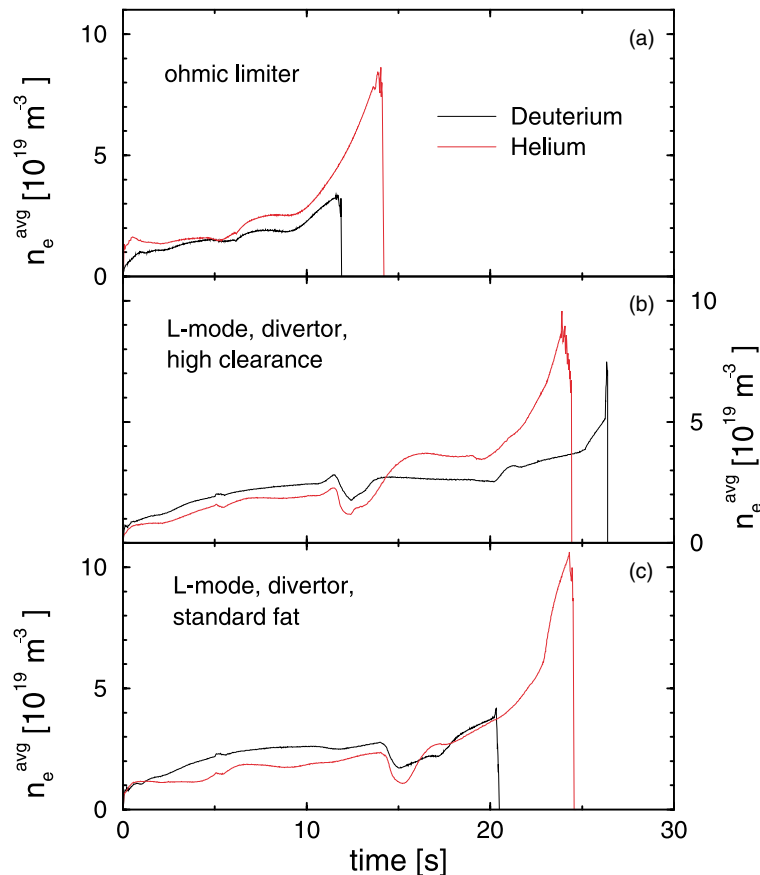


Fig. 1. Overview of L-mode density limits: (a) ohmic, limiter 1.8 MA, 2.8 T (#44819, #53995), (b) high clearance, diverted, 1.7 MA, 2.4 T, $P_{\text{NBI}} = 2 \text{ MW}$ (#53080, #54030), (c) standard fat, diverted, 2 MA, 2.4 T, $P_{\text{NBI}} = 2.3 \text{ MW}$ (#53088, #54029).

strongly after the radiation zone has moved inside the LCFS. In standard fat configuration the difference in the density limits is even more pronounced. In the case of

the helium plasma (#54029) a density of factor $2.8\times$ the maximum density in the deuterium case (#53088) can be found (see Fig. 1(c)). This is mostly due to the fact that

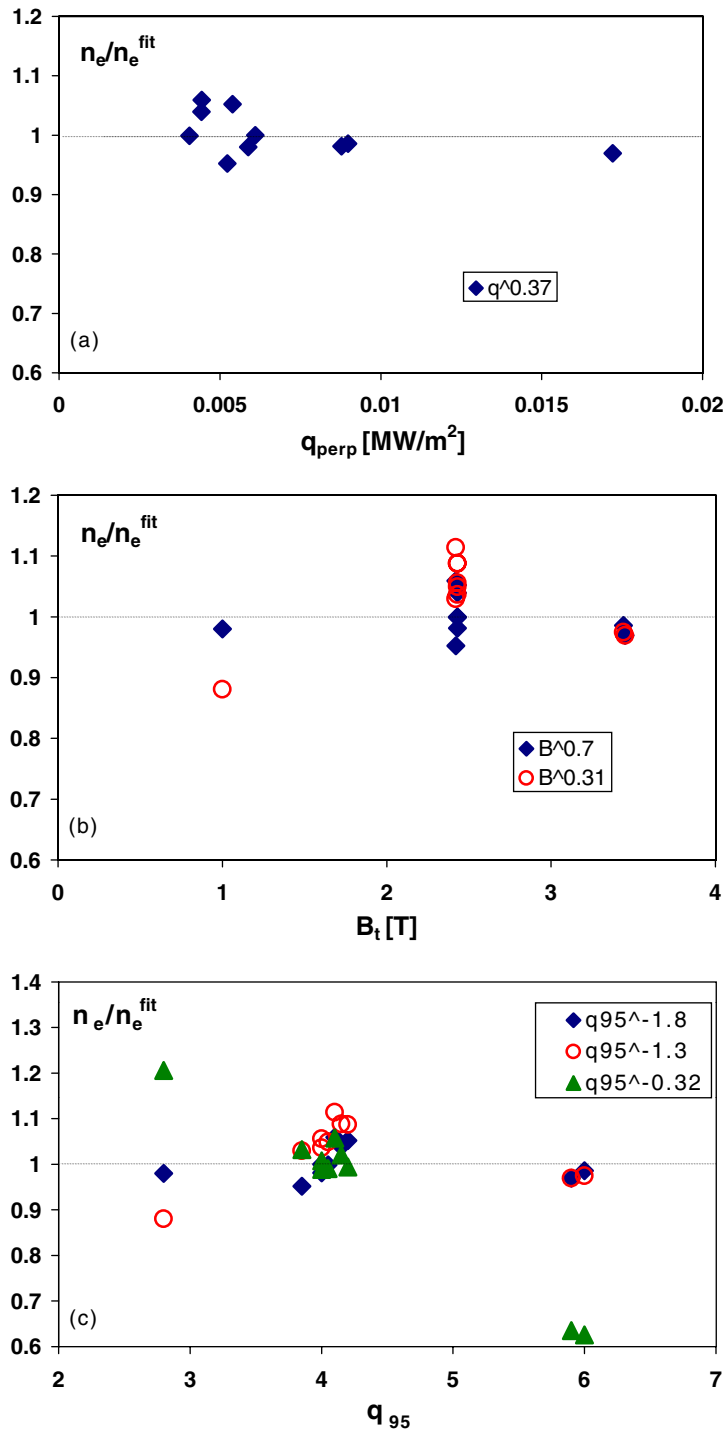


Fig. 2. Comparison of different scalings for the X-point MARFE onset: (a) scaling versus heat flux crossing LCFS, (b) scaling versus toroidal magnetic field, (c) scaling versus edge safety factor.

in deuterium for low wall clearance (standard fat configuration) the onset of the wall MARFE happens to be at almost the same density as for the X-point MARFE and thus at a lower density [4].

While in the deuterium discharges the inner divertor is completely detached just before the X-point MARFE formation [4], particle detachment in helium discharges is only obtained close to the radiative collapse ($f_{\text{rad}} = 100\%$). There are no indications of volume recombination [5] at the highest densities and divertor temperatures of ≈ 4 eV, which is consistent with the fact that no particle detachment is observed (see also [6]).

The divertor closure has no influence on the density limit. Also no difference in the density limit has been encountered, when puffing from the inner or outer divertor. This is different from the deuterium density limits [4], in which the onset of the X-point MARFE depends on the puffing location and the divertor closure.

A series of L-mode density limit experiments have been performed in which the parameter range was varied largely: B_t between 1 and 3.4 T; q_{\perp} between 0.0027 MW/m² and 0.017 MW/m²; I_p between 1 and 2 MA; q_{95} between 2.6 and 3.3. For the onset of the X-point MARFE or more exactly, for the density when the radiation zone moves inside the LCFS an empirical scaling for the line-averaged density can be found (see Fig. 2): $\bar{n}_e^{\text{XPM}} \propto q_{\perp}^{0.37} B_t^{0.7} (q_{95}R)^{-1.8}$. No difference in the density profiles in the SOL between deuterium and helium, as measured by a Li-beam, has been observed [7].

The onset of the X-point MARFE in deuterium density limits has been described successfully by a model based on divertor detachment [8]. Although the difference in the onset of the X-point MARFE between deuterium and helium is relatively small, the scaling of the X-point MARFE onset predicted by [8], $\bar{n}_e^{\text{XPM}} \propto n_s^{\text{det}} \propto q_{\perp}^x B_t^{0.31} (q_{95}R)^{x-0.69}$, does not agree with the He experiments (with $x = 0.37$ determined from power scan) as it can be seen in Fig. 2. However, accepting a larger error bar $\bar{n}_e^{\text{XPM}} \propto q_{\perp}^{0.37} B_t^{0.31} (q_{95}R)^{-1.3}$ would lead to a reasonable fit of the experimental data. Although Bohm-like transport would be consistent with this scaling, a larger dependence on the edge safety factor remains. This could be due to the fact that the helium ionisation front is at higher temperatures, when compared to deuterium, and a different mechanism, like the thermal condensation process, could be relevant for the triggering of MARFEs.

Since one of the main differences between deuterium and helium plasmas is the development of inner wall MARFEs, a test of relevant theories is mandatory. For the trigger of the inner MARFE an instability has been proposed [9], which is based on localised recycling. The critical density for the development of this instability is:

$$n_b^{\text{cr}} \approx \frac{1}{q_b} \sqrt{\frac{\kappa_{\parallel} \alpha}{60\pi R D_{\perp} \sigma_{\text{at}}}} \quad (2)$$

with $\sigma_{\text{at}} = \sqrt{k_i(k_i + k_c)}/v_a$ [10]. The ionisation rate coefficient k_i changes by a factor of 2–3, in the temperature interval of 20–70 eV and density of $\approx 2 \times 10^{19}$ m⁻³. Those boundary values for T_e and n_e are consistent with results from EDGE2D simulations. The charge exchange rate coefficient k_c changes by a factor of ≈ 12 for temperatures above 10 eV, where the main charge exchange process is $\text{He} + \text{He}^{2+} \rightarrow \text{He}^{2+} + \text{He}$. Hence, in the further consideration charge exchange processes are neglected. For deuterium the charge exchange rate coefficient is in the same order as the ionisation rate coefficient. The velocity $v_a = (T/m_i)^{1/2}$ should be reduced in helium by factor $\sqrt{2}$, however there is an indication that the energy of the helium neutrals is larger than that of deuterium (≈ 20 eV for helium and ≈ 4 eV for deuterium on average [7]). Altogether, including the change in v_a by a factor of 1.6 this reduces σ_{at} for helium by a factor of ≈ 6.7 (with $k_i^{\text{D}}/k_i^{\text{He}} = 3$). Additionally, the change in $\kappa_{\parallel} \propto 1/(Z_{\text{eff}} \ln A)$ has to be taken into account. While helium density limit discharges (divertor L-mode) are very clean with a $Z_{\text{eff}} \approx 2$ deuterium density limit discharges (divertor L-mode) have typically a $Z_{\text{eff}} \approx 1.4$. This could lead to an increase in the critical density for the onset of the recycling instability by a factor 2.2. Here it was assumed that D_{\perp} is independent on the mass and charge (Bohm-like or constant). The impurity radiation would change the critical density slightly. For deuterium the critical density is about 20% lower, when carbon radiation is taking into account [11–13]. Note that $n_c/n_e = 0.5\%$, which is a typical carbon concentration in L-mode density limits, radiates as much as $n_{\text{He}}/n_e = 50\%$. So, qualitatively taking into account radiation does not change the conclusion.

2. H-mode density limit

Since the L to H power threshold is higher in helium plasmas than in deuterium plasmas and the recycling of helium is much different from deuterium, a fair comparison of these plasmas is difficult. Fig. 3 shows a comparison of the H-mode density limits. The H-mode density limit is defined here by the H to L backtransition, which is followed by the development of an X-point MARFE and finally disrupts in L-mode. The transition from type-I ELMs to type-III ELMs is not discussed in this paper. The line-averaged density is approximately 10–15% higher in helium than in deuterium before the H to L backtransition. However, a closer look at the density profiles reveals that the pedestal density is the same for both gases, since the density profile is peaked. This might be due to the different beam fuelling rates. Due to the elevated H-mode power threshold the heating power of helium H-mode discharges had to be increased (see Fig. 3(b)). Thus in helium, particle fuelling with neutral beams is 3.5 times

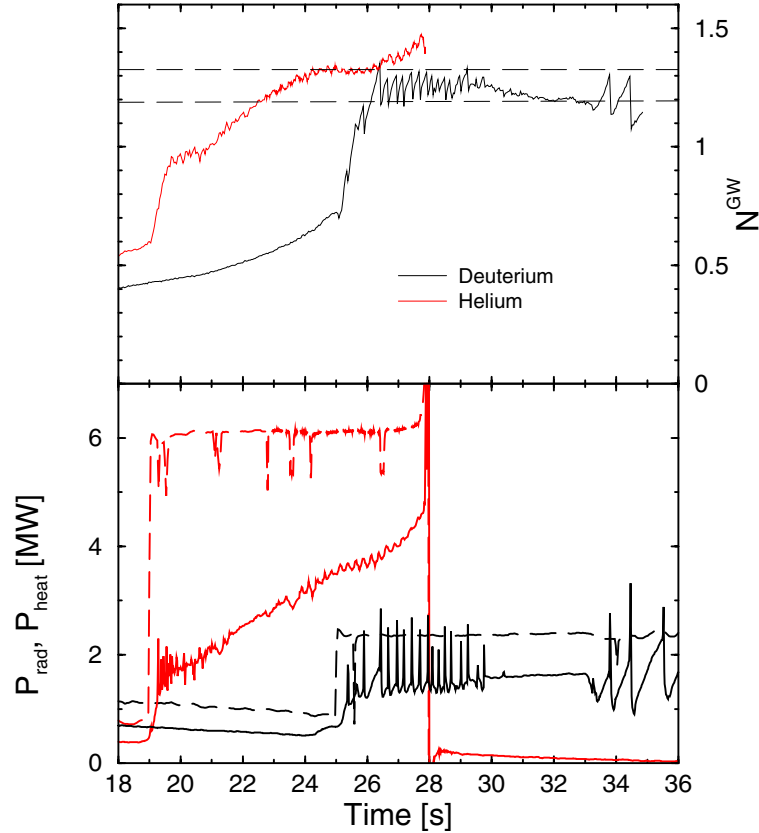


Fig. 3. Comparison of H-mode density limit in deuterium (0.94 MA, 1 T) and helium (1 MA, 1 T): (a) line-averaged density normalised to Greenwald-density, the horizontal lines indicate the maximum density, in the case of helium it is the H to L backtransition, where it is in the case of deuterium the maximum density in type-III ELMy H-mode (see also [14]), (b) heating and radiated power.

higher than in the deuterium pulse, leading to seven times higher electron fuelling. The peaking cannot be due to the ware pinch ($v_r = -E_\phi/B_\theta$), since the loop voltage is the same for both cases (He and D). Often the H-mode density limit is said to be linked to the divertor detachment. However, a close look to the detachment process during the H to L backtransition reveals that the inner divertor stays completely attached during the whole process.

As for the L-mode density limit, the parameter dependence of the H-mode density has been investigated. A proper regression analysis of the H-mode density limit in helium is not possible due to the sparse data, but it is instructive to compare the helium H-mode density limit with predicted scaling [15], which fitted the empirical scalings found for the H-mode density limit in deuterium very well: $n_e^{BLS} = \bar{n}_e = n_e^{ped} = 41.4 \times q_\perp^{0.09} B_t^{0.53} (q_{95}R)^{-0.88}$ where n_e is in 10^{19} m^{-3} , q_\perp in MW/m^2 , B_t in T and R in m. In Fig. 4 the pedestal density at the H to L transition is compared with the above scaling for deuterium. In addition to the points relating to H to L transitions, points from high density discharges are shown. The data points

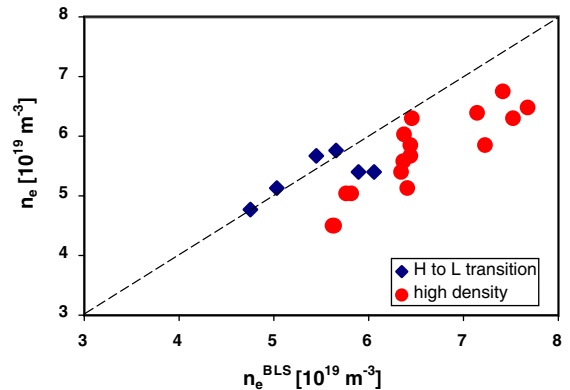


Fig. 4. Comparison of the helium H-mode density limits (H to L transition) with the scaling (n_e^{BLS}) found for deuterium H-mode density limits; additionally high density helium plasmas are compared.

from high density discharges are lower in absolute values than the prediction as expected, but follow the

scaling. In general there is a reasonable agreement between the scaling and the absolute values derived from deuterium H-mode density limit and the helium H-mode density limit.

The H-mode density limit in deuterium was also explained by a theory describing the density limit as a result of divertor detachment [15]. However, the helium L-mode density limit was not predictable by the theory based on detachment. One reason for this could be that the cooling of the X-point in the helium discharges is not sufficient to trigger the X-point MARFE but it is enough to destroy the H-mode. The second reason could be that the H-mode density limit is rather driven by plasma core physics.

3. Conclusions

L-mode density limit: The X-point MARFE onset in helium L-mode plasmas is slightly higher than in comparable deuterium discharges. The final, maximum density can be increased by a factor 2.8. This is mainly due to the fact that the helium density limit discharge does not encounter an inner wall MARFE but rather experiences a poloidal symmetric radiative collapse. This can be explained by the reduction of the ionisation rate coefficient and the negligible combined charge exchange and elastic rate coefficients together with the increased energy of the neutrals (helium). This leads to an increased penetration depth of the neutrals, which avoids the formation of a wall MARFE as consequence of a recycling instability. In addition ohmic heating is more efficient in the case of helium, which leads to higher heating powers and consequently high densities for the

radiative collapse. The H-mode density limit in helium is the same as for deuterium.

References

- [1] B. Lipschultz, *J. Nucl. Mater.* 145–147 (1987) 15.
- [2] ITER Physics Expert Groups on Confinement and Transport and Confinement Modeling and Database, and ITER Physics Basics Editors, *Nucl. Fusion* 39 (1999) 2175.
- [3] J. Wesson, *Tokamaks*, Clarendon, Oxford, 1987.
- [4] J. Rapp et al., *Proceedings of the 28th Conference on Plasma Physics and Controlled Fusion*, Funchal, Portugal, *Europhys. Conf. Abstr.*, 2001.
- [5] A. Meigs, private communication.
- [6] A. Loarte, *Contrib. Plasma Phys.* 40 (2000) 3–4.
- [7] A. Korotkov, private communication.
- [8] K. Borrass, R. Schneider, R. Farengo, *Nucl. Fusion* 37 (4) (1997) 523.
- [9] M.Z. Tokar' et al., *J. Nucl. Mater.* 266–269 (1999) 958.
- [10] M.Z. Tokar', *Plasma Phys. Control. Fusion* 35 (1993) 1119.
- [11] D. Reiser et al., *Proceedings of the 26th International Conference on Plasma Physics and Controlled Fusion*, Maastricht, The Netherlands, *Europhys. Conf. Abstr.* 23J (1999) 697.
- [12] R. Zagórski et al., *Contrib. Plasma Phys.* 40 (3–4) (2000) 405.
- [13] D. Reiser, M.Z. Tokar', *Proceedings of the 25th International Conference on Plasma Physics and Controlled Fusion*, Prague, Czech Republic, *Europhys. Conf. Abstr.* 22C (1998) 1828.
- [14] K. Borrass et al., *Proceedings of the 28th Conference on Plasma Physics and Controlled Fusion*, Funchal, Portugal, *Europhys. Conf. Abstr.*, 2001.
- [15] K. Borrass, J. Lingertat, R. Schneider, *Contrib. Plasma Phys.* 38 (1/2) (1998) 130.